Electronic Supporting Information

Remarkable Activity and Stability of Photocatalytic Hydrogen Production over Dye-Sensitized Single Molecular Layer MoS$_2$ Ensemble

Experimental

Preparation of S-MoS$_2$

Single-layer MoS$_2$ was synthesized by the exfoliation of MoS$_2$ with lithium intercalation[1]. The starting material used in the reported studies was bulk MoS$_2$ powder from Sigma Aldrich. 500 mg of the black MoS$_2$ powder was first soaked in 8 mL of 1.6 M n-butyl lithium in hexane for 48 hours under nitrogen atmosphere. Following the intercalation of the MoS$_2$ by lithium, the produced Li$_x$MoS$_2$ was washed repeatedly with hexane to remove the excess butyl-lithium and dried under nitrogen atmosphere. Then the powder was immersed in water and the suspension was ultrasonicated during the reaction to assist in the exfoliation. It was assumed that the reaction between the water and the intercalated lithium forms hydrogen gas between the layers, and the expansion of this gas tends to separate the MoS$_2$ layers. As the reaction proceeded more deeply into each crystallite, the layers became further separated. Eventually the layers became completely separated and remain suspended in the aqueous solution. The pH of this solution was basic due to the presence of lithium hydroxide.

Synthesis of S-MoS$_2$/graphene

S-MoS$_2$/Graphene was prepared by ultrasonication and stirring method at room temperature. Graphene oxide (GO) was synthesized from natural graphite powder by a modified Hummers' method[2]. 10 mL of 1 mg/mL graphite oxide was first ultra sonicated in ethanol for 1 hour. 10 mL of 2 mg/mL exfoliated MoS$_2$ suspension was then added to graphene oxide solution slowly under sonication, and the mixture

continued to be sonicated for 1 hour. After that, the mixed solution was stirred at room temperature for 24 hours to obtain uniform solution.

Synthesis of M-MoS$_2$

In a typical synthesis of multi-layer MoS$_2$[3], 1 mmol (241.95 mg) of Na$_2$MoO$_4 \bullet$ 2H$_2$O and 5 mmol (380.6 mg) of thiourea were dissolved in 60 mL of distilled water. The solution was sonicated 30 minutes until a homogeneous solution was obtained. Then, it was transferred into a 125 mL Teflon-lined autoclave and held at 210 °C for 24 hours. During the process, Na$_2$MoO$_4 \bullet$2H$_2$O was reduced to well-crystallized MoS$_2$ using thiourea as a source of sulfur and also a reductant. After that, the black precipitate was collected by centrifugation, washed three times with deionized water and ethanol, and then dried in an oven at 80 °C for 12 hours.

Synthesis of M-MoS$_2$/graphene

According to the above TEM (Fig. S1) the deposition of S-MoS$_2$ can well be dispersed on graphene in solvent through sonication however this could not be done in the case of M-MoS$_2$. Thus, M-MoS$_2$/graphene hybrids were prepared by a routine hydrothermal method[3]. 1 mmol of Na$_2$MoO$_4 \bullet$2H$_2$O and 5 mmol of thiourea were dissolved in 60 mL of distilled water, and then the prepared GO was added into the solution. The solution was sonicated for 30 minutes until a homogeneous solution was obtained. After that, it was transferred into a 125 mL Teflon-lined autoclave and held at 210 °C for 24 hours. After the reaction, the black precipitate was collected by centrifugation, washed three times with deionized water and ethanol, and then dried in an oven at 80 °C for 12 hours. During the hydrothermal process, graphene oxide was converted to reduced graphene oxide (RGO), and MoS$_2$ was deposited on RGO at the

same time. Here, the existence of graphene oxide facilitates the dispersion of M-MoS_2.

Photocatalytic measurements

The photocatalytic H_2 evolution experiments were performed in a 250 mL sealed Pyrex flask. As for the photocatalytic reaction of S-MoS_2, different amounts of exfoliated suspension were dispersed in 100 mL aqueous solution with 15% (v/v) triethanolamine as a sacrificial reagent by sonication for 30 minutes. The flask was thoroughly purged with 5%CH_4/Argon mixed gas for 30 minutes to remove air. The reaction was irradiated under the 500 W Xe lamp with constant stirring. Finally, 30 mL of evolved gas were manually collected from the headspace of the flask and analyzed in Agilent 7980 gas chromatograph. In the EY-sensitized system, different amounts of EY were added to the suspension with water and triethanolamine and further sonicated for another 15 minutes before bubbling with 5% CH_4/Argon mixed gas.

It is noted that the photocatalytic activity depends on quantum efficiency which in turn depends on nature of photosensitive species and particular wavelength used. Different wavelengths should be studied if a fair comparison is made between different photosensitive species. But the main focus of this communication note is to show the high activity of S-MoS_2 compared to bulk or multilayer MoS_2 as photo-catalyst. We were therefore systematically comparing the activity of different forms of MoS_2 without adding CdS and other photosensitive components as promoters in this paper with no intention to compare our S-MoS_2 samples with reported multi-component systems involving different photosensitive species or co-catalysts in the literature.
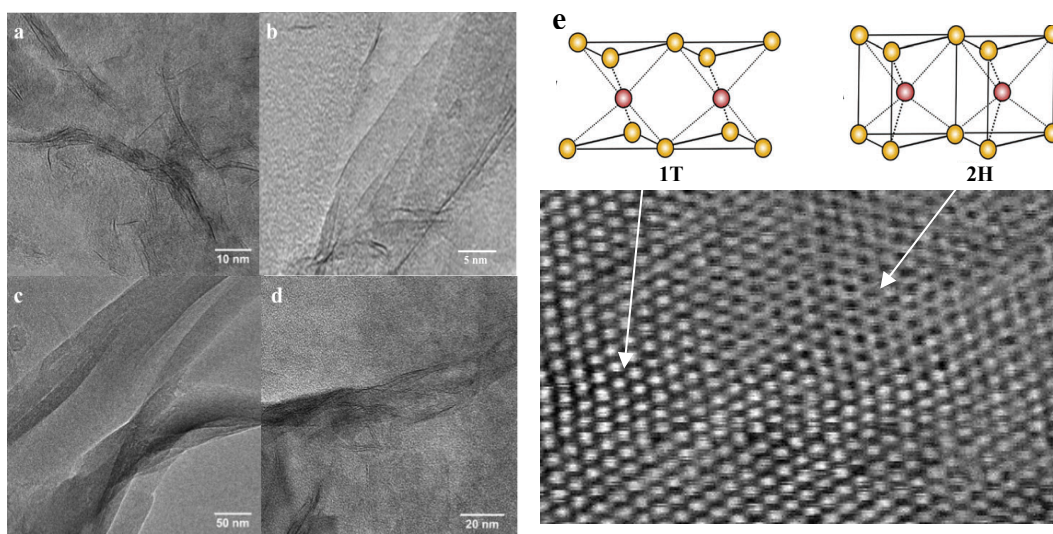
Figure S1. TEM images of thin 2-D fakes of S-MoS$_2$ (a, b) and S-MoS$_2$/graphene (c, d) Enlarged STEM image of a region of a single-layer MoS$_2$ with co-existence of 2H (right) and 1T (left) phases is observed.
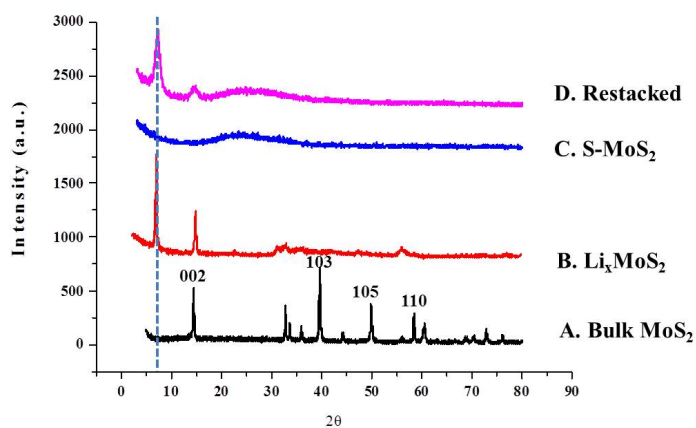
Figure S2. X-ray diffraction patterns for bulk MoS$_2$ (A), LixMoS$_2$ (B), exfoliated single-layer MoS$_2$ in suspension (C) and restacked single-layer MoS$_2$ (D)
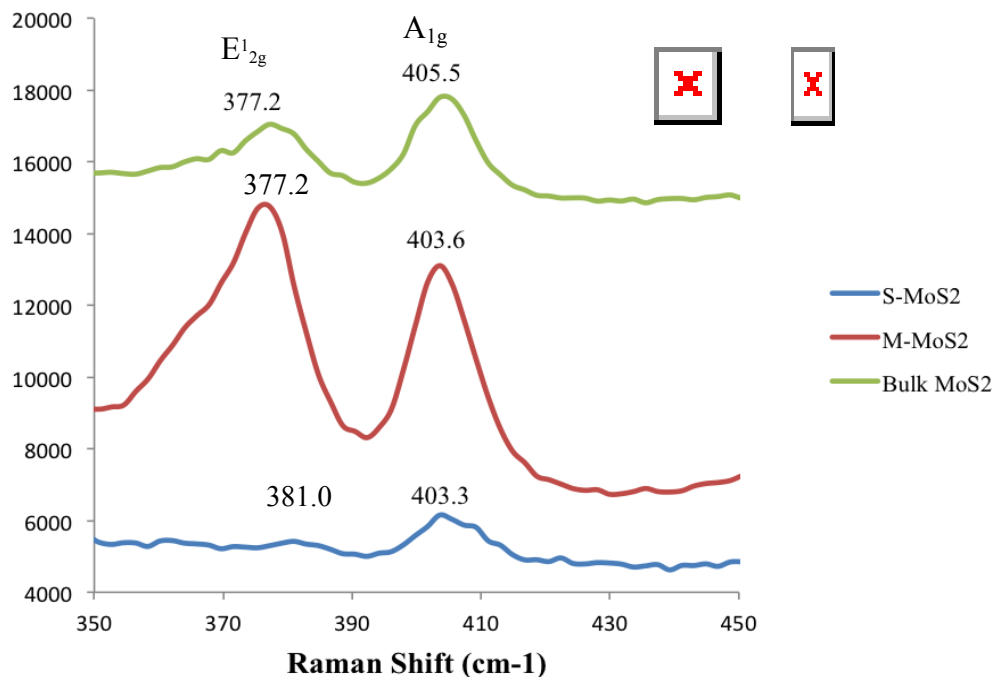
Figure S3. Raman spectra of bulk MoS_2, M-MoS_2 and S-MoS_2.

X-ray diffraction patterns for bulk MoS_2, Li_xMoS_2, single layer MoS_2 by fast solvent removal and restacked MoS_2 (slow removal of solvent) were also collected and are shown in Fig. S2, respectively. For bulk MoS_2 (Fig. S2a), the typical peaks at 2θ = 14.2°, 33.0°, 38.2°, 49.2°, 58.9°, and 69.8° can be attributed to the (002), (100), (103), (105), (110) and (201) planes of hexagonal 2H-MoS_2, and the strong (002) peak with a d-spacing of 6.12 Å signifies a well-stacked layered structure along the c axis[25]. In the XRD pattern of Li_xMoS_2, there is a new peak at 7.93° appearing due to expanded lattice expansion. The (002) peak vanishes completely from Li-intercalated sample in aqueous phase (exfoliation) forming dispersed single layers after the fast solvent removal (Fig. S2c). The Raman spectroscopy characterization of this sample (Fig. S3) is also in consistent with the single molecular layer of 1T MoS_2 [25]. Fig. S2d shows the pattern for a restacked of exfoliated sample upon slow solvent removal with observable peaks at 7.4° (c = 11.14 Å) and 14.8° (c = 5.97 Å), which are attributed to the (001) and

(002) reflections of MoS_2 layers, giving a spacing between Mo layers of 11.14 Å (matched with the reported 1-T MoS_2[25]). This corresponds to each layer of MoS_2 hosts an adsorbed monolayer of water approximately 2.6 Å thick, and the layers are re-stacked [25]. This suggests that the exfoliated single molecular MoS_2 in hydrated form is highly unstable again re-stacking when without water stabilization. It is known that the Raman spectrum of bulk MoS_2 shows two prominent peaks: an in-plane (E^1_{2g}) mode located at around 377.2 cm^{-1} and an out-of-plane (A_{1g}) mode located at 405.5 cm^{-1} (Figure S6). The in-plane mode corresponds to the sulphur atoms vibrating in one direction and the molybdenum atom in the other direction, while the out-of-plane mode is a mode of just the sulphur atoms vibrating out of the plane[4]. The E^1_{2g} phonon stiffens with decreasing number of layers and a blue shift of the peak from 377.2 cm^{-1} of multi-layers to 381.0 cm^{-1} of monolayer MoS_2 occurs. On the other hand, A_{1g} phonon softens with decreasing number of layers, giving rise to a slight red shift from 405.5 cm^{-1} of bulk material to 403.3 cm^{-1} of monolayer. As the numbers of MoS_2 layers drop, these two modes could be used to monitor the change in the layer thickness. Thus, the difference of these two modes may be used as a mean to measure the degree of monolayer MoS_2 formation according to literature[4]. However, due to local variations in film thickness, rotational stacking disorder and slight shift in frequencies of these Raman modes, they do not seem to allow direct determination of the number of layers in our samples. Further work would be needed in this area to address the quantitative analysis.
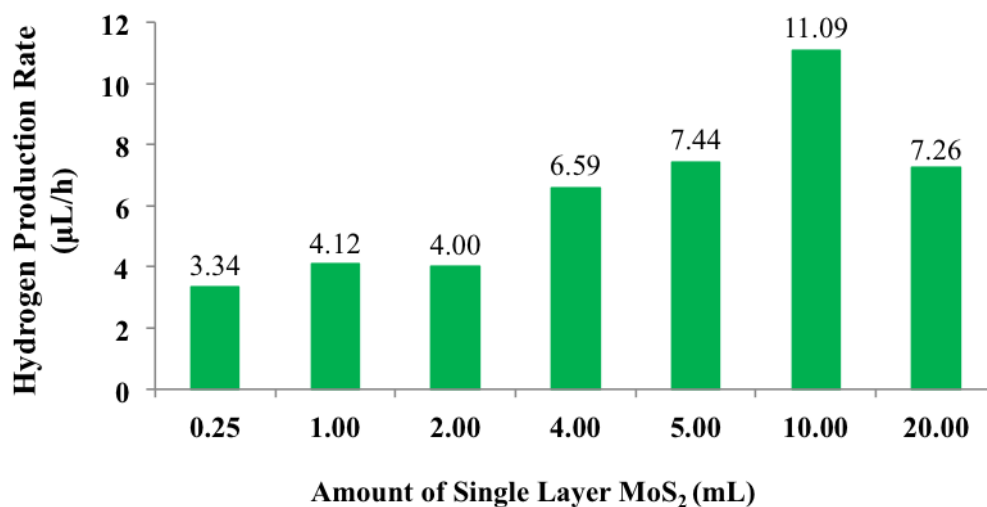
Figure S4. Photocatalytic hydrogen production as a function of S-MoS$_2$ quantity in 100 mL H$_2$O with 15% (v/v) TEOA aqueous solution under 500 W UV irradiation for 2 hours.
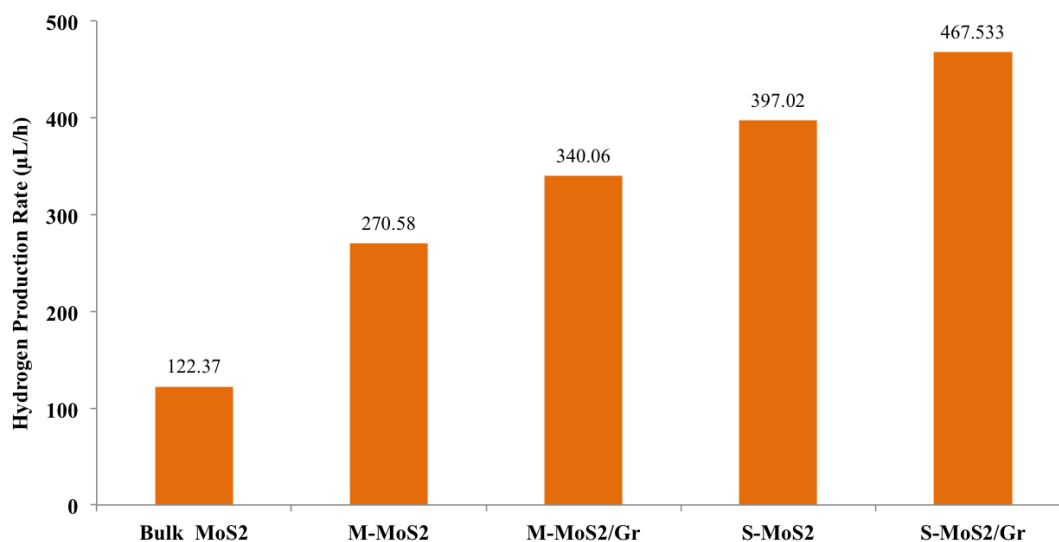
Figure S5. Hydrogen evolution from EY photosensitized systems catalyzed by bulk MoS$_2$, M-MoS$_2$, S-MoS$_2$, M-MoS$_2$/graphene, S-MoS$_2$ graphene in 100 mL of 15% (v/v) TEOA aqueous solution under UV irradiation.
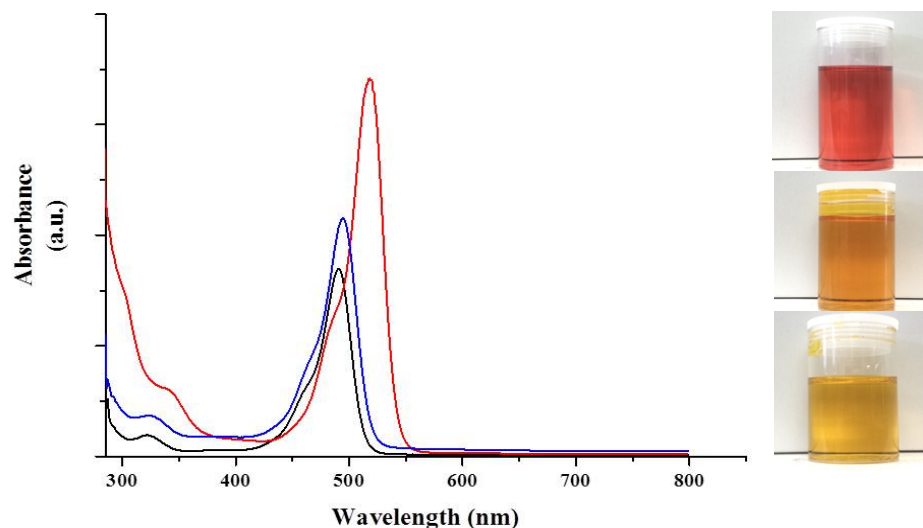
Figure S6. UV-Vis absorption spectra of EY sensitized M-MoS$_2$/graphene solution in 15% (v/v) TEOA aqueous solution after 0, 4, 8 hours of photoreactions showing the decolorization of EY by shifting the peak maxima to the shorter wavelength. M-MoS$_2$/graphene was removed by centrifugation before UV-Vis analysis.
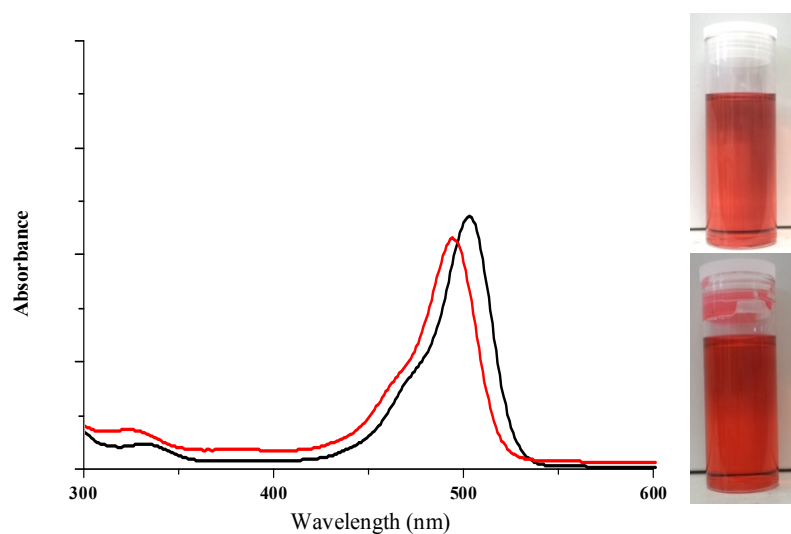
Figure S7. UV-Vis absorption spectra of EY sensitized S-MoS$_2$ solution in 15% (v/v) TEOA aqueous solution before and after 20 hours of photoreactions (no colour change). the colloidal stable S-MoS$_2$ was still well dispersed in solution.
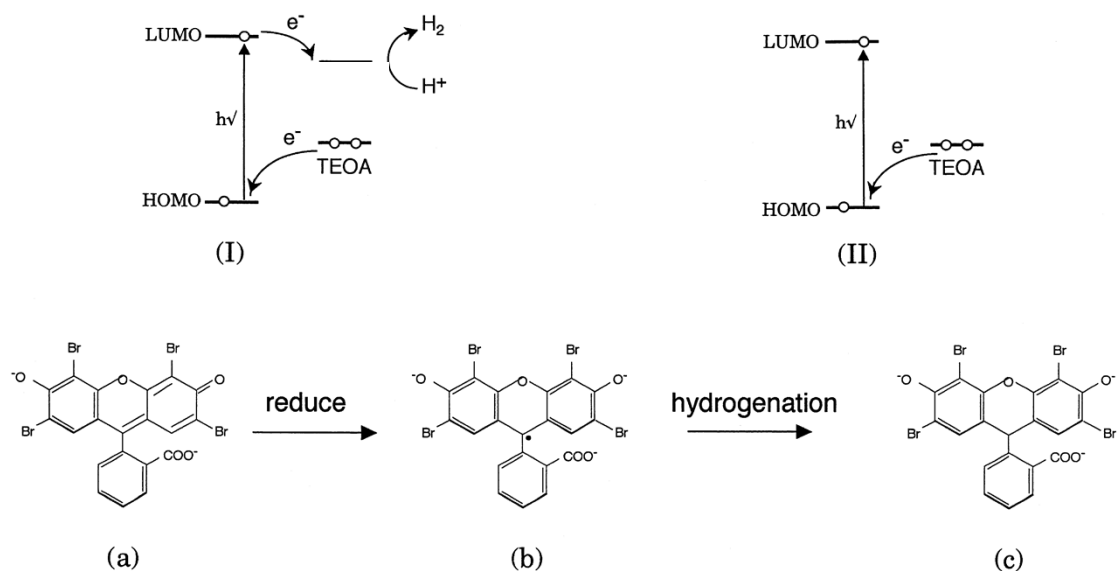
Figure S8. Proposed photoelectron transfer (I) on dye molecules at the solution–semiconductor interface and (II) on dye molecules free in solution. Structure of (a) Eosin Y and (b) one-electron reduced species and (c) Eosin Y formed by further reduction or disproportionation leading to its decolouration (c)[5].
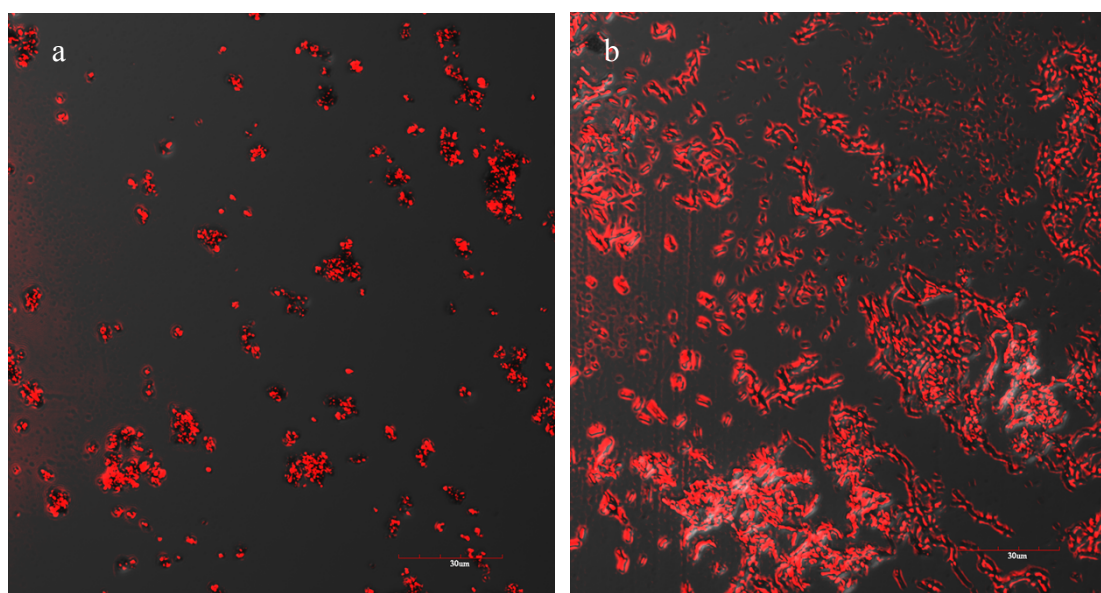
Figure S9. A confocal microscopy of EY molecules (at 590-610 nm) on M-MoS$_2$ (a) and S-MoS$_2$ (b) collected at the same parameters (1:1) mass ratio of EY to MoS$_2$, each 1.00 mg was sonicated in 100 μl ethanol with extensive rinsing with ethanol; few drops to slide until air dried); same magnification with the scale bar of 30 μm.
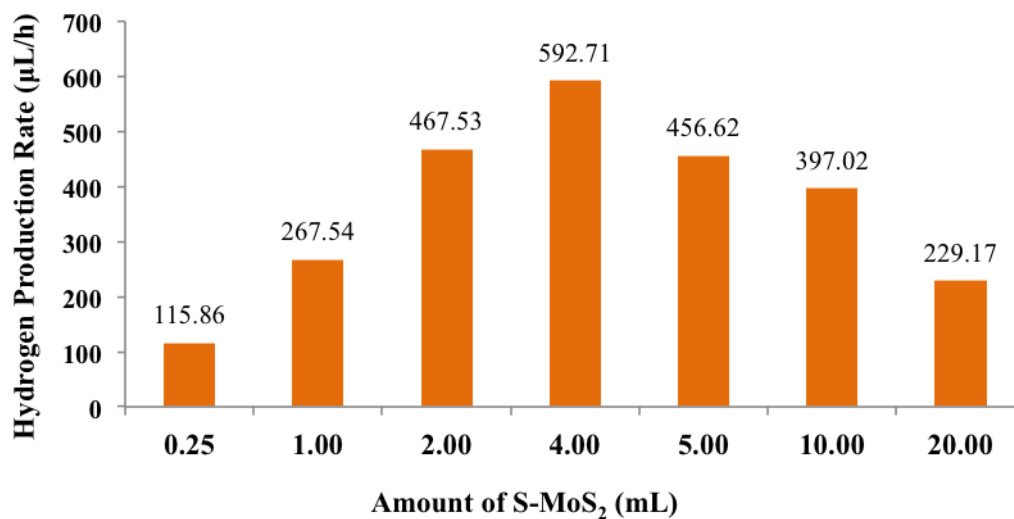
Figure S10. Hydrogen evolution over EY (4.0×10^{-4} M) sensitized with different amount of S-MoS$_2$ (2 mg/mL) in 100 mL of 15% TEOA aqueous solution under 500 W UV irradiation for 2 hours.
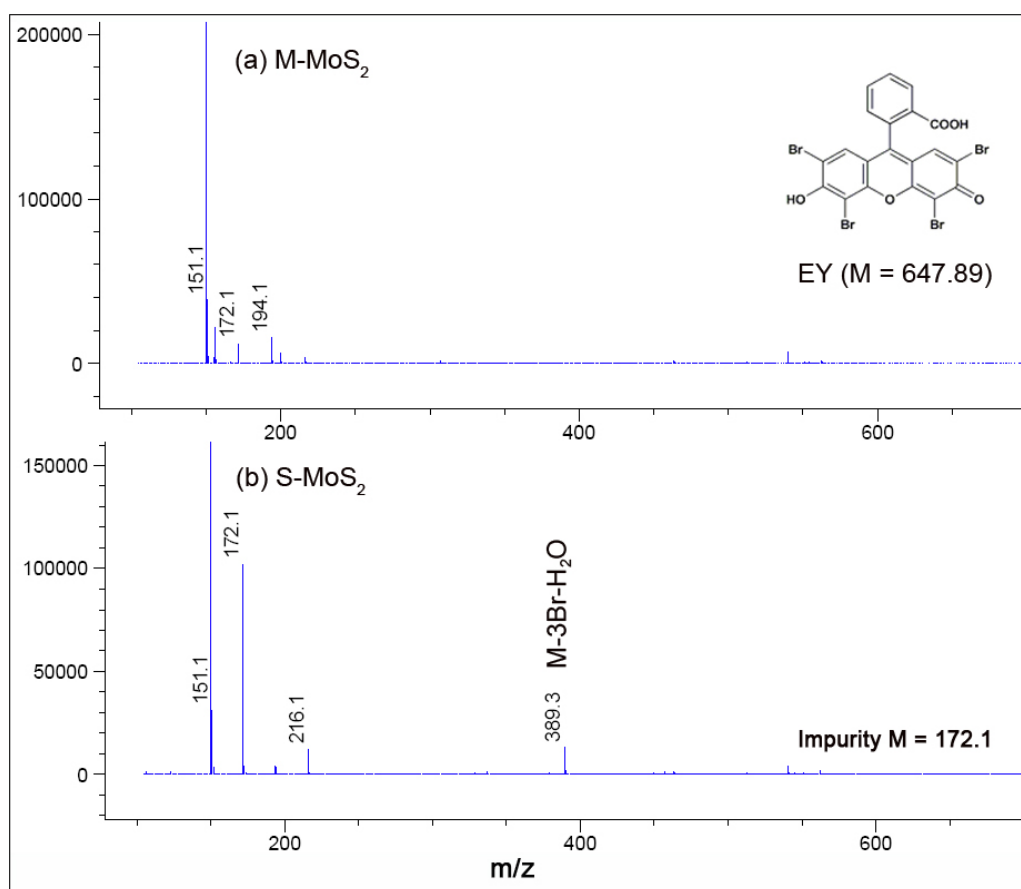
Figure S11. Mass spectra of mixture after reaction with Eosin Y molecules (a) M-MoS$_2$ and (b) S-MoS$_2$
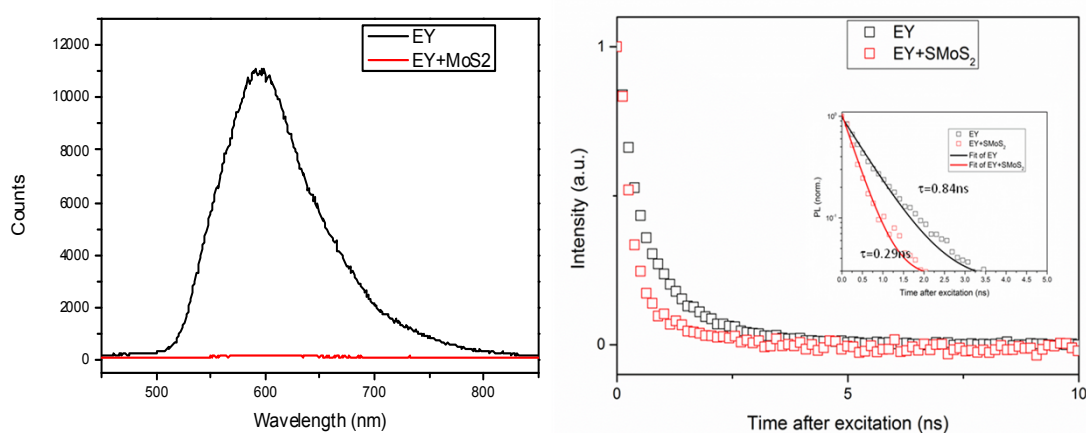
Figure S12. Static (left) and Time-resolved Photoluminescence (right) of Eosin Y and Eosin Y/S-MoS$_2$ on glass slide excited using a 405 nm laser pulsed at frequencies of 32 MHZ.

Steady-state and time-resolved Photoluminescence (PL) measurements were acquired using a time-correlated single photon counting (TCSPC) setup (FluoTime 300, PicoQuant GmbH). Samples were excited using a 405nm laser pulsed at frequencies of 32MHz. The PL was collected using a high resolution monochromator and hybrid photomultiplier detector assembly (PMA Hybrid 40, PicoQuant GmbH). Parameters describing the photoluminescence were obtained by fitting the background-corrected PL with a stretched exponential decay function of the form y = A1*exp(-x/t1) + y0. Errors in the fitting parameters were determined by examining the Adjusted R-squares obtained by independently varying each fitting parameter. For ease of comparison of lifetimes between samples with different quenchers, τ1 is defined as the time taken after excitation for the PL intensity to drop to 1/e of its peak intensity (see Tables S1 &2).

Table S1 Fitting result-EY

Model	ExpDec1		
Equation	y = A1*exp(-x/t1) + y0		
Reduced Chi-Sqr	5.60601E-5		
Adj. R-Square	0.99625		
		Value	Standard Error
EY	y0	0.01007	0.0017
	A1	0.77599	0.01282
	t1	0.84366	0.0169
	k	1.18531	0.02375
	tau	0.58478	0.01172

Table S2 Fitting result-EY+SMoS$_2$

Model	ExpDec1		
Equation	y = A1*exp(-x/t1) + y0		
Adj. R-Square	0.99247		
		Value	Standard Error
EY+SMoS2	y0	0.03488	0.00484
	A1	1.20832	0.03819
	t1	0.29271	0.01191
	k	3.41635	0.13904
	tau	0.20289	0.00826

Computational Details

All calculations were performed in the framework of DFT by using the Vienna ab initio simulation package (VASP)[6-9]. The projector-augmented wave (PAW) potentials [10,11] were used for the core electron interaction. The Perdew–Burke–Ernzerhof (PBE) functional [12,13] based on the generalized gradient approximation (GGA) was employed to evaluate the non-local exchange-correlation energy. A plane wave basis set with a cutoff energy of 350 eV was used. For structure optimization, the ionic positions were allowed to relax until the forces were less than 0.05 eV/Å. Spin polarization is included for all the calculations. The k-point grid determined by the Monkhorst-Pack method was 9×9×2 for the bulk calculations in this study. The value of our optimized lattice paramter for bulk MoS$_2$ are a = 3.193 Å, c = 12.611 Å with a layer thickness of 3.153 Å (S − S vertical distance). The adsorptions on MoS$_2$(0001) single layer were carried out using a p(6×6) supercell and a k-point grid of 2×2×1 while the MoS$_2$(10**Error!**0) surface was modeled by a p(5×2) supercell with six atomic layers while the k-point grid was 2×1×1 and the bottom three were fixed during all the calculations. A vacuum layer of 20 Å along the z direction

perpendicular to the surface (the x and y directions being parallel to the surface) was employed to prevent spurious interactions between the repeated slabs. The adsorption energy is calculated as:

$$E_{ads} = -(E_{slab+EY} - (E_{slab} + E_{EY}))$$

While the $E_{slab+EY}$ indicated the total energy of adsorbed structure, the E_{slab} and E_{EY} was the total energy of the clean surface of MoS_2 and the Eosin Y (EY) molecule, respectively. The H atom of hydroxyl and carboxyl groups in Eosin Y could dissociate in solution to form EY^{2-}. On $MoS_2(0001)$ surface, when the EY^{2-} adsorbed it could abstract the nearby surface H to form neutral EY molecule and the adsorption energy is 0.06 eV. On the other hand, at $MoS_2(10\textbf{Error!}0)$ the exposed Mo edge could give strong binding with the ionized carboxyl groups meanwhile the C-Br bond could also be broken and left Br atom on the surface. Due to the breaking bonds, the adsorption energy at $MoS_2(10\textbf{Error!}0)$ Mo edge could be as high as 6.49 eV.

Optimized configuration of EY on MoS2(0001) basal plane
(a,b)

Optimized configuration of EY on MoS2(1010) basal plane
(c,d)
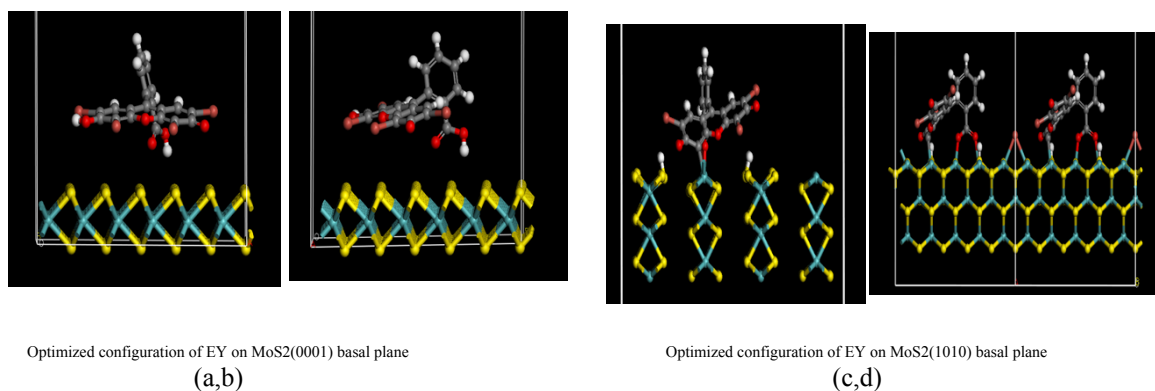
Figure S13. DFT optimization of Eosin Y on $MoS_2(0001)$ (a,b) and $MoS_2(10\textbf{Error!}0)$ (c,d).

Thus, as stated in the main text, EY as a photosensitizer has been extensively studied in the literature. Our static and time-resolved photo-luminescence (PL) spectroscopies are consistent with the literature that there is a transfer of photo-induced electron from EY to $S-MoS_2$ (see Fig. 4b in the main text). The presence of sulphur vacancies upon Li treatment can be reflected from our EDX analysis and observed phase transition (2H to 1T). The significance of high degree of sulphur vacancies in monlayer MoS_2 is also recently discussed [14,15]. Although we have not yet had a direct compelling evidence on Lewis acid-base linkage between the EY and $S-MoS_2$ at present, our circumstantial evidence from theoretical calculations and the detection of C-Br cleavage from EY upon interaction with $S-MoS_2$ could indicate such bonding formation. In addition, the recent demonstration of a facile route of using thiol or

related compounds to repair sulphur vacancies through covalent bonding formation [15] and the agrument for Lewis acid-base linkage in the case of EY-ZnO (reference 29 in main text) are also well accepted in the literature. This clearly infers the formation of the strong interaction between the EY molecule with the S-MoS$_2$, giving remarkable photocatalytic performance.

[1] P. Joensen, R. F. Frindt, S. R. Morrison, *Mater. Res. Bull.* **1986**, 21, 457.

[2] D. C. Marcano, D. V. Kosynkin, J. M. Tour *et al*. *ACS. Nano* **2012**, 4, 4806.

[3] Q. Xiang, J. Yu, M. Jaromiec. *J. Am. Chem. Soc.* **2012**, 134, 6575.

[4] K. F. Mak, C. Lee, J. Hone, J. Shan, T. F. Heinz, *Phys. Rev. Lett.* **2010**, 105, 136805.

[5] R. Abe et al. J. Photochem. Photobio. A: Chem **2000**, 137, 63.

[6] G. Kresse and J. Hafner.. Phys. Rev. B, 47:558, 1993.

[7] G. Kresse and J. Hafner. Phys. Rev. B, 49:14251, 1994.

[8] G. Kresse and J. Furthmüller. Comput. Mat. Sci., 6:15, 1996.

[9] G. Kresse and J. Furthmüller. Phys. Rev. B, 54:11169, 1996.

[10] P. E. Blochl. Phys. Rev. B, 59:1758, 1999.

[12] J. P. Perdew, K. Burke, and M. Ernzerhof. Phys. Rev. Lett., 77:3865, 1996.

[13] J. P. Perdew, K. Burke, and M. Ernzerhof. Phys. Rev. Lett., 78:1396, 1997.

[14] S. Chou, et al., JACS 135, 4584, 2013.

[15] Z. Yu, et al., Nature Communications 6290, 2014.